Assimilation of geomagnetic observations in dynamical models of the Earth's core

Alexandre Fournier & Julien Aubert

Institut de Physique du Globe de Paris
research supported by the CNES, INSU (LEFE-ASSIM program), GENCI-IDRIS (Grant 2011-042122)
calculs effectués sur le centre de calcul de l'IPGP, S-CAPAD, et sur VARGAS

Journée ORAP, 14 octobre 2011

Outline

Outline

- Geomagnetic data provided over the last decade by satellites (and used in conjunction with observatory data) have allowed us to get a more accurate description of the rapid variations of the main geomagnetic field (generated inside earth's core)
- This better description is an incentive for constructing and testing physical models of core dynamics able to account for the observed geomagnetic variations (in a data assimilation framework).

$$\begin{aligned}\mathbf{B} &= -\boldsymbol{\nabla} V \text{ in a current-free region,}\\ V(\mathbf{r},t) &= a\sum_{\ell,m}\left(\frac{a}{r}\right)^{\ell+1}\left[g_\ell^m(t)\cos m\varphi + h_\ell^m(t)\sin m\varphi\right] P_\ell^m(\cos\theta),\\ B_r(\mathbf{r},t) &= \sum_{\ell,m}\left(\frac{a}{r}\right)^{\ell+2}\left[g_\ell^m(t)\cos m\varphi + h_\ell^m(t)\sin m\varphi\right] P_\ell^m(\cos\theta).\end{aligned}$$

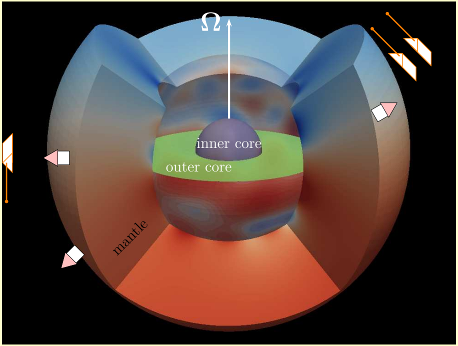

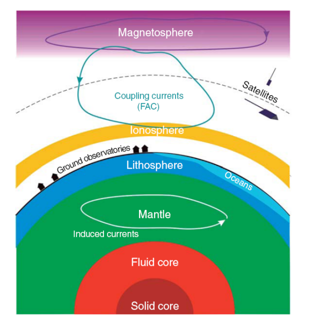

Figure 1 Sketch of the various sources contributing to the near-Earth magnetic field.

Hulot, Sabaka, Olsen TOG 2007

Geomagnetic observations are connected with the (large-scale) radial component of the magnetic induction, B_r, at the core surface (the small scales are screened by the crustal field).

B_r (nT) at Earth's surface in 2007

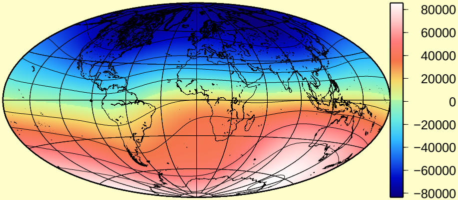

B_r (nT) at the core surface in 2007

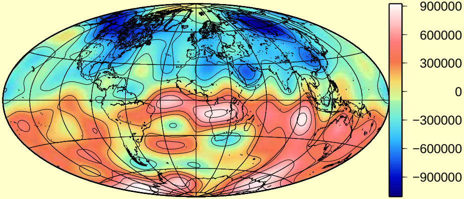

Mauersberger–Lowes spectrum

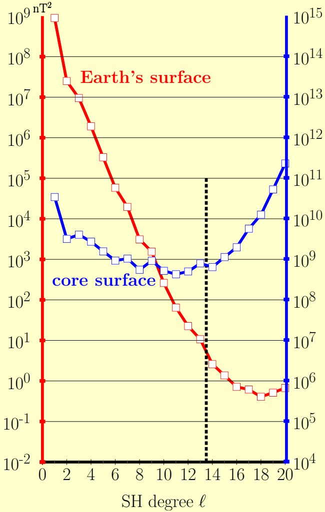

CHAOS2 model (1997-2009), Olsen et al., GJI, 2009

$\dot{B}_r$ (nT/y) at Earth's surface in 2007

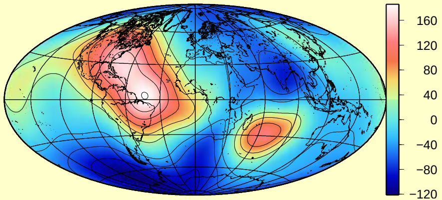

$\dot{B}_r$ (nT/y) at the core surface in 2007

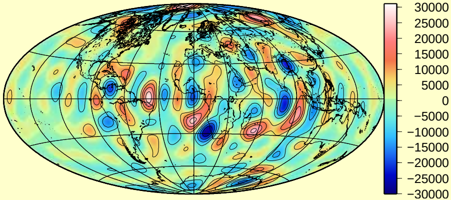

Mauersberger-Lowes spectrum

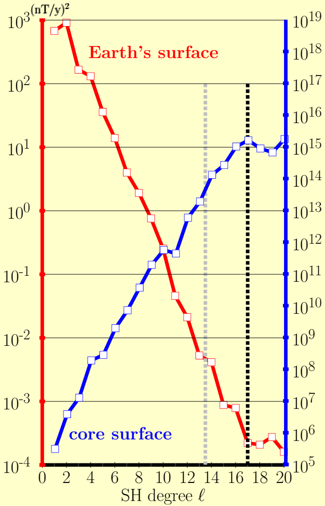

CHAOS2 model (1997-2009), Olsen et al., GJI, 2009

Instantaneous correlation times **(Hulot & Le Mouël, PEPI, 1994)**

$$\tau_\ell(t) = \sqrt{\frac{\sum_{m=0}^{\ell} g_\ell^m(t)^2 + h_\ell^m(t)^2}{\sum_{m=0}^{\ell} \dot{g}_\ell^m(t)^2 + \dot{h}_\ell^m(t)^2}}$$

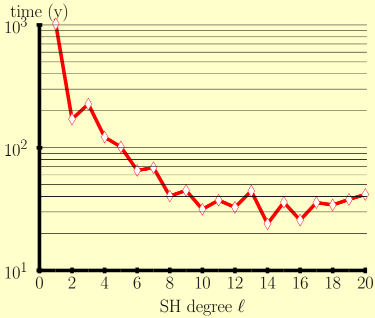

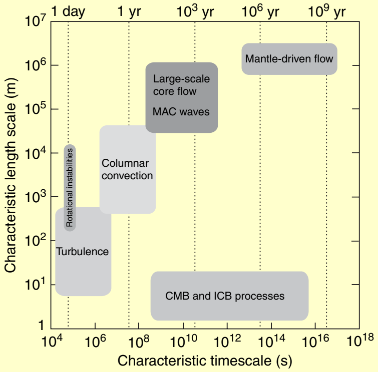

Figure 15 Spectra of characteristic length and timescales in core dynamics. MAC – Magnetic, Archimedean, Coriolis waves.

Olson, TOG, 2007

Data distribution vs. time: increase in quantity and accuracy

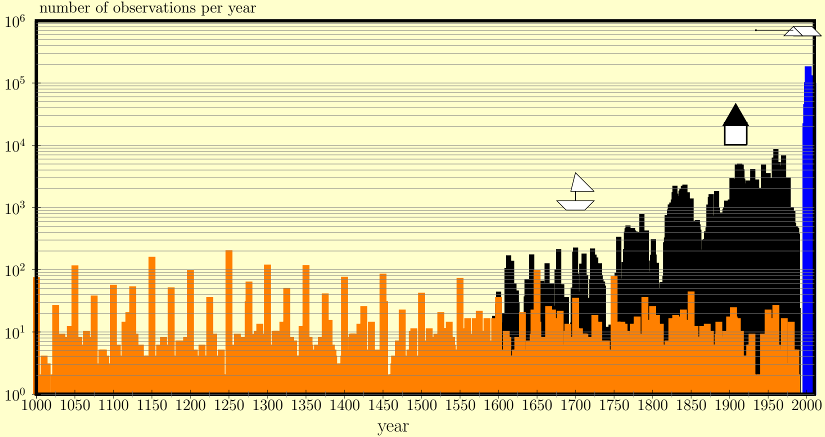

(Fournier et al., Space Sci. Rev., 2010)

archeomagnetic data (orange): geomagia database **(Donadini et al., G^3, 2009)**; historical data (black): *gufm1* **(Jackson et al., PhilTrans,2000)**; satellite data (blue): xCHAOS **(Olsen & Mandea, NGEO, 2008)**.

Satellite data make a difference: error in geomagnetic field models

0.02 $(\mathrm{nT/y})^2$ for CHAOS vs. $\sim 30\ (\mathrm{nT/y})^2$ in the 1980ies (Hulot et al., TOG, 2007).

Kinematic approach : seek the (large scale) core surface flow $\mathbf{u}_h$ such that

$$\partial_t B_r = \dot{B}_r = -\boldsymbol{\nabla}_h \cdot (\mathbf{u}_h B_r)?$$

- Frozen-flux approximation **(Roberts & Scott, JGG, 1965)**,
- Non-uniqueness. Extra hypotheses required: steady flow **(Voorhies & Backus, GAFD, 1985)**, tangencial geostrophy **(Le Mouël, Nature, 1984)**, quasi-geostrophy **(Pais & Jault, GJI, 2008; Gillet et al., G^3, 2009)**, $\ldots +$ regularization **(Holme, TOG, 2007, for a recent review)**
- Spatial resolution error $\gg$ observation error.

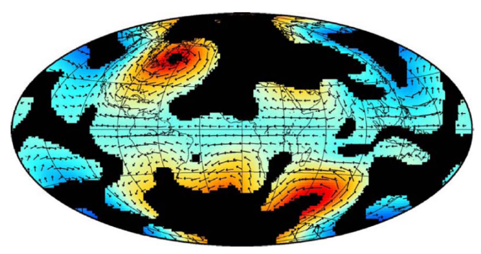

Eymin & Hulot, PEPI, 2005. Peak velocity: 37 km/y. Pressure (color): $\pm$1010 Pa.

A dynamical approach to the inverse problem of estimating the state of the core $\mathbf{x}$ is in order (e.g. Talagrand, JMSJ, 1997, for a review on assimilation).

Ingredients:

1. observations
2. a dynamical model describing the physics of the processes under scrutiny

Goals:

- Probe the physics governing the secular variation: advection, hydromagnetic waves, with an ounce (or more) of diffusion **(e.g. Hide, PhilTrans, 1966; Finlay & Jackson, Science, 2003; Gubbins, PEPI, 1996; Chulliat & Olsen, JGR, 2010)** Important because fundamental
- Make inferences on the interior of the core
- Retro-propagate the current quality of observations **(Fournier et al., NPG, 2007)**
- Increase the quality of the geomagnetic forecast, and assess its limits **(e.g. Kuang, Tangborn, et al., GJI, 2009; EPS, 2010)**

Specific to the core problem ($\neq$ meteorology, oceanography)

- 'Surface' measurements only
- uncertainties in the knowledge of the background state (the 'climatological' mean)

Outline

Discretization of conservation laws and Maxwell's equations, modified Boussinesq codensity formalism of Braginsky & Roberts (GAFD, 1995).

$$\nabla \cdot \mathbf{u} = 0, \tag{1}$$

Discretization of conservation laws and Maxwell's equations, modified Boussinesq codensity formalism of Braginsky & Roberts (GAFD, 1995).

$$
\begin{aligned}
\boldsymbol{\nabla} \cdot \mathbf{u} &= 0, && (1)\\
\rho \left(\partial_t \mathbf{u} + \mathbf{u} \cdot \boldsymbol{\nabla} \mathbf{u} + 2\boldsymbol{\Omega} \times \mathbf{u} \right) &= -\boldsymbol{\nabla} \Pi + \mathbf{j} \times \mathbf{B} + \rho\nu\nabla^2 \mathbf{u} + C\mathbf{g}, && (2)
\end{aligned}
$$

Discretization of conservation laws and Maxwell's equations, modified Boussinesq codensity formalism of **Braginsky & Roberts (GAFD, 1995)**.

$$
\begin{aligned}
\boldsymbol{\nabla} \cdot \mathbf{u} &= 0, & (1)\\
\rho \left(\partial_t \mathbf{u} + \mathbf{u} \cdot \boldsymbol{\nabla} \mathbf{u} + 2\boldsymbol{\Omega} \times \mathbf{u}\right) &= -\boldsymbol{\nabla} \Pi + \mathbf{j} \times \mathbf{B} + \rho\nu\nabla^2 \mathbf{u} + C\mathbf{g}, & (2)\\
\partial_t C + \mathbf{u} \cdot \boldsymbol{\nabla} C &= \kappa \nabla^2 C + S_{T/\xi}, & (3)
\end{aligned}
$$

Discretization of conservation laws and Maxwell's equations, modified Boussinesq codensity formalism of **Braginsky & Roberts (GAFD, 1995)**.

$$
\begin{aligned}
\boldsymbol{\nabla}\cdot\mathbf{u} &= 0, && (1)\\
\rho\left(\partial_t\mathbf{u}+\mathbf{u}\cdot\boldsymbol{\nabla}\mathbf{u}+2\boldsymbol{\Omega}\times\mathbf{u}\right) &= -\boldsymbol{\nabla}\Pi+\mathbf{j}\times\mathbf{B}+\rho\nu\nabla^2\mathbf{u}+C\mathbf{g}, && (2)\\
\partial_t C+\mathbf{u}\cdot\boldsymbol{\nabla}C &= \kappa\nabla^2 C+S_{T/\xi}, && (3)\\
\partial_t\mathbf{B} &= \boldsymbol{\nabla}\times(\mathbf{u}\times\mathbf{B})+(1/\mu\sigma)\nabla^2\mathbf{B},
\end{aligned}
$$

Discretization of conservation laws and Maxwell's equations, modified Boussinesq codensity formalism of Braginsky & Roberts (GAFD, 1995).

$$
\begin{aligned}
\boldsymbol{\nabla} \cdot \mathbf{u} &= 0, && (1)\\
\rho\left(\partial_t \mathbf{u} + \mathbf{u} \cdot \boldsymbol{\nabla} \mathbf{u} + 2\boldsymbol{\Omega} \times \mathbf{u}\right) &= -\boldsymbol{\nabla}\Pi + \mathbf{j} \times \mathbf{B} + \rho\nu\nabla^2\mathbf{u} + C\mathbf{g}, && (2)\\
\partial_t C + \mathbf{u} \cdot \boldsymbol{\nabla} C &= \kappa\nabla^2 C + S_{T/\xi}, && (3)\\
\partial_t \mathbf{B} &= \boldsymbol{\nabla} \times (\mathbf{u} \times \mathbf{B}) + (1/\mu\sigma)\nabla^2\mathbf{B}, && (4)
\end{aligned}
$$

+ no-slip boundary conditions for $\mathbf{u}$, insulating magnetic boundary conditions at the ICB and CMB, prescribed codensity at the ICB and null codensity flux $\boldsymbol{\nabla} C = \mathbf{0}$ at the CMB.

Numerical approach: the PARODY code

Authors

Emmanuel Dormy, Julien Aubert, Philippe Cardin
(and later collaborative developments).

Numerical scheme based on **Glatzmaier (Journal of Computational Physics, 1984)**.

- poloidal-toroidal decomposition of **u** and **B**

$$\begin{aligned}\mathbf{u} &= \nabla \times \nabla \times (u_P \mathbf{r}) + \nabla \times (u_T \mathbf{r}),\\ \mathbf{B} &= \nabla \times \nabla \times (B_P \mathbf{r}) + \nabla \times (B_T \mathbf{r}).\end{aligned}$$

- Spherical harmonic expansion of u_P, u_T, B_P, B_T, and C

$$\begin{bmatrix} u_P \\ u_T \\ B_P \\ B_T \\ C \end{bmatrix} (r, \theta, \phi, t) = \sum_{\ell=0}^{l=L} \sum_{m=-\ell}^{m=\ell} \begin{bmatrix} u_{P\,\ell m}(r,t) \\ u_{T\,\ell m}(r,t) \\ B_{P\,\ell m}(r,t) \\ B_{T\,\ell m}(r,t) \\ C_{\ell m}(r,t) \end{bmatrix} \mathcal{Y}_\ell^m(\theta, \phi)$$

- Finite differences in radius r
- Computation of nonlinear terms in physical space
- Second order semi-implicit time-differencing

Dormy, Cardin, Jault, EPSL, 1998; Aubert, Aurnou, Wicht, GJI, 2008

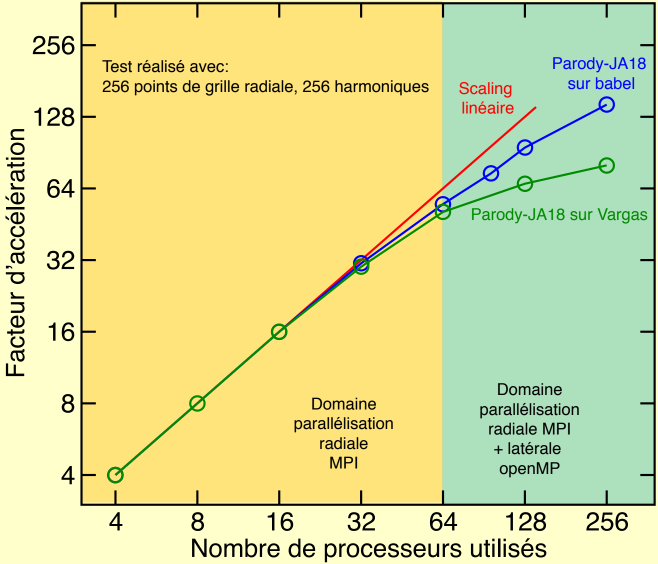
Test réalisé avec:
256 points de grille radiale, 256 harmoniques
Scaling linéaire
Parody-JA18 sur babel
Parody-JA18 sur Vargas
Domaine parallélisation radiale MPI
Domaine parallélisation radiale MPI + latérale openMP
Facteur d'accélération
Nombre de processeurs utilisés
4
8
16
32
64
128
256

Difficulties

Simulations are overdiffusive ; time scales are not in appropriate proportions

Table 1

Dynamo parameters α thermal expansivity, g_o gravity at core surface, ΔT superadiabatic temperature contrast across core, κ thermal diffusivity, ν kinematic viscosity, Ω rotation rate, D outer core thickness, $\eta = 1/(\mu_o\sigma)$ magnetic diffusivity with σ electrical conductivity and μ_o magnetic permeability, U characteristic flow velocity, B characteristic magnetic field strength, ρ density, Ra_c is the critical Rayleigh number for onset of convection.

	Control parameters			
	Rayleigh no.	Ekman no.	Magn. Prandtl no.	Prandtl no.
Definition	$Ra = \alpha g_o \Delta T/(\Omega^2 D)$	$E = \nu/(\Omega D)^2$	$Pm = \nu/\eta$	$Pr = \nu/\kappa$
Core	$10^4 Ra_c$	$10^{-15} - 10^{-14}$	$10^{-6} - 10^{-5}$	0.1–1
Models	$(1 - 100)Ra_c$	$10^{-3} - 10^{-6}$	0.1–10	1
	Diagnostic numbers			
	Magn. Reynolds no.	Reynolds no.	Rossby no.	Elsasser no.
Definition	$Rm = UD/\eta$	$Re = UD/\nu$	$Ro = U/(\Omega D)$	$\Lambda = B^2/(2\mu_o \eta \rho \Omega)$
Core	10^3	10^9	10^{-7}	0.1–10
Models	40–2000	< 2000	$10^{-2} - 10^{-4}$	0.1–100

Christensen, PEPI, 2011

We use scaling laws to exptrapolate model values to geophysical values.

B_r@CMB, filtered @ $\ell = 13$

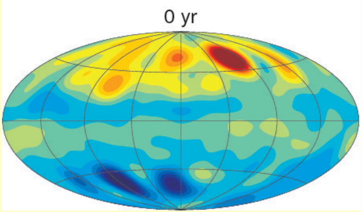

M1

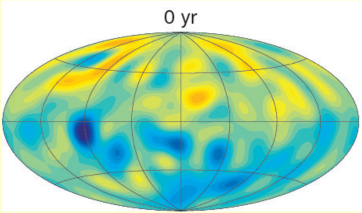

M3

	Rm	E_η	Pm	rating
M1	100	$2.5\ 10^{-4}$	4	6
M3	860	$1.25\ 10^{-5}$	2.5	1

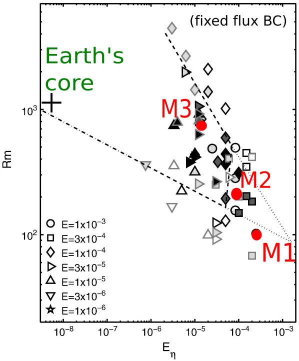

After Christensen, Aubert, Hulot (EPSL, 2010)

B_r@CMB, scale : ± 2 mT

M1

M3

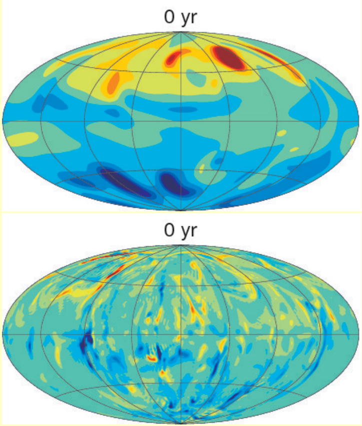

	Rm	E_η	Pm	rating
M1	100	2.5 10^{-4}	4	6
M3	860	1.25 10^{-5}	2.5	1

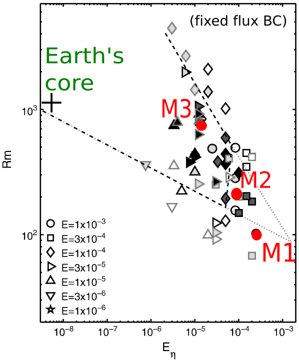

After Christensen, Aubert, Hulot (EPSL, 2010)

2 dynamo models

B_r@CMB, scale : ± 2 mT

	Rm	E_η	Pm	rating
M1	100	$2.5\ 10^{-4}$	4	6
M3	860	$1.25\ 10^{-5}$	2.5	1

M1

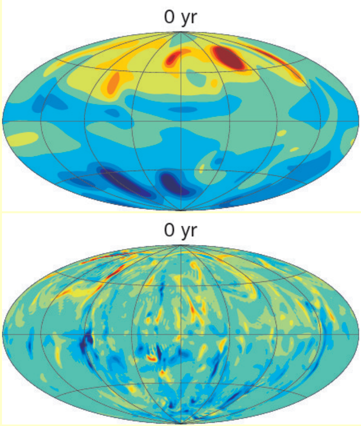

M3

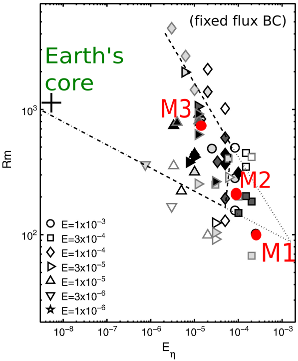

After Christensen, Aubert, Hulot (EPSL, 2010)

Surface and volume

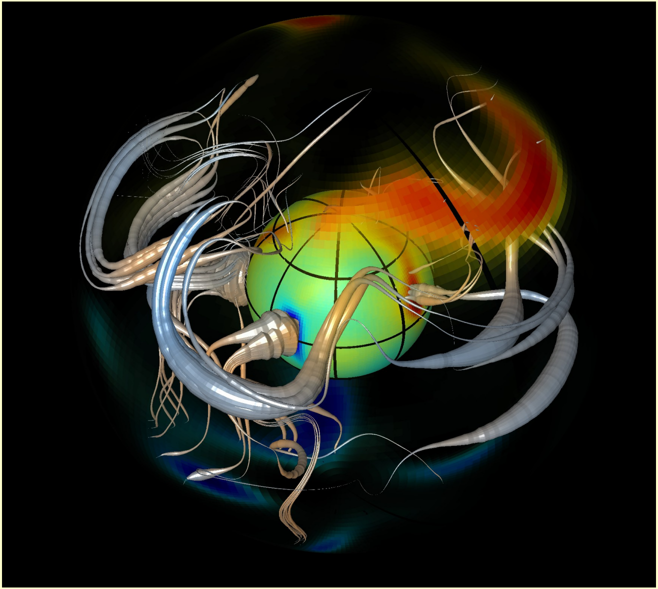

Dynamic Magnetic Field Imaging: Aubert, Aurnou, Wicht (GJI, 2008)

Outline

Trajectory in model space

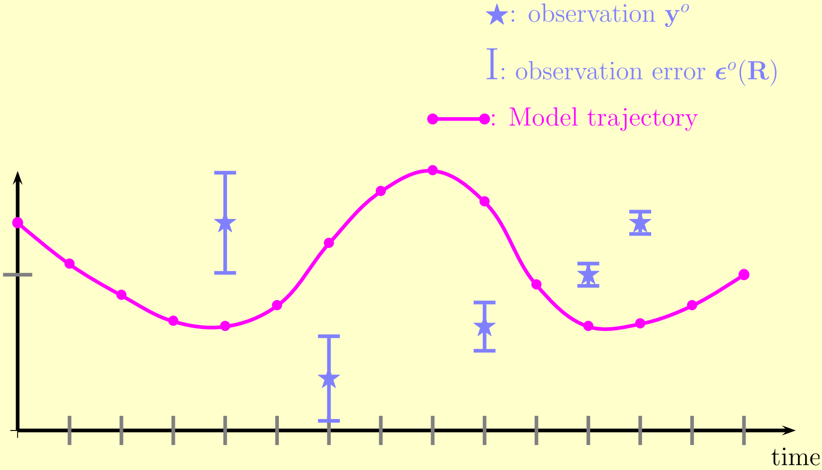

We perform an analysis each time there is some observation available.

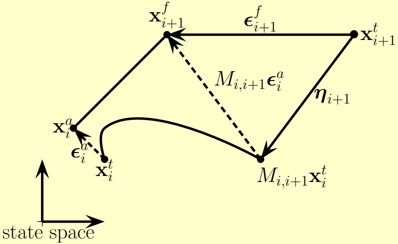

A 2-step procedure: the Kalman filter

1. Forecast:

$$\begin{aligned} \mathbf{x}^f_{i+1} &= M\mathbf{x}^a_i, \\ \mathbf{P}^f_{i+1} &= M\mathbf{P}^a_i M^\dagger + \mathbf{Q}. \end{aligned}$$

2. Analysis:

$$\begin{aligned} \mathbf{x}^a_{i+1} &= \mathbf{x}^f_{i+1} + \mathbf{K}_{i+1}\left(\mathbf{y}^o_{i+1} - \mathbf{H}\mathbf{x}^f_{i+1}\right), \\ \mathbf{P}^a_{i+1} &= \left(I - \mathbf{K}_{i+1}\mathbf{H}\right)\mathbf{P}^f_{i+1}. \end{aligned}$$

with $\mathbf{K}_{i+1} = \mathbf{P}^f_{i+1}\mathbf{H}^\dagger_{i+1}\left(\mathbf{H}_{i+1}\mathbf{P}^f_{i+1}\mathbf{H}^\dagger_{i+1} + \mathbf{R}_{i+1}\right)^{-1}$.

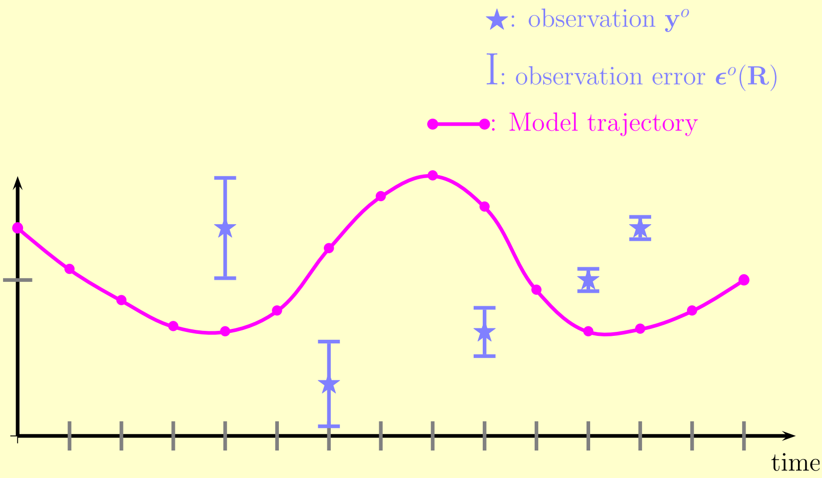
★: observation $\mathbf{y}^o$
I: observation error $\boldsymbol{\epsilon}^o(\mathbf{R})$
: Model trajectory
time

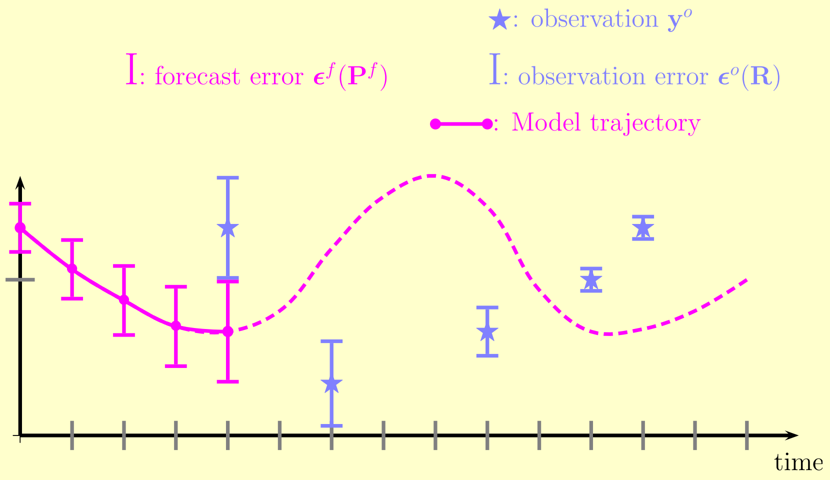
★: observation $\mathbf{y}^o$
I: forecast error $\boldsymbol{\epsilon}^f(\mathbf{P}^f)$
I: observation error $\boldsymbol{\epsilon}^o(\mathbf{R})$
: Model trajectory
time

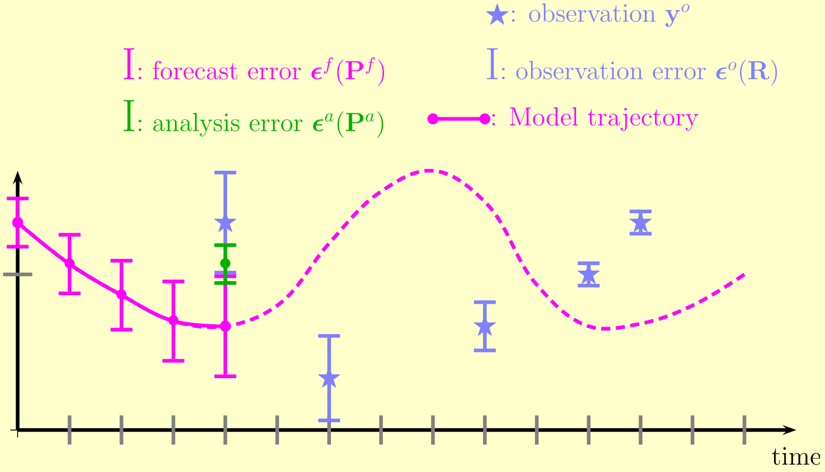
★: observation $\mathbf{y}^o$
I: forecast error $\boldsymbol{\epsilon}^f(\mathbf{P}^f)$
I: observation error $\boldsymbol{\epsilon}^o(\mathbf{R})$
I: analysis error $\boldsymbol{\epsilon}^a(\mathbf{P}^a)$
: Model trajectory
time

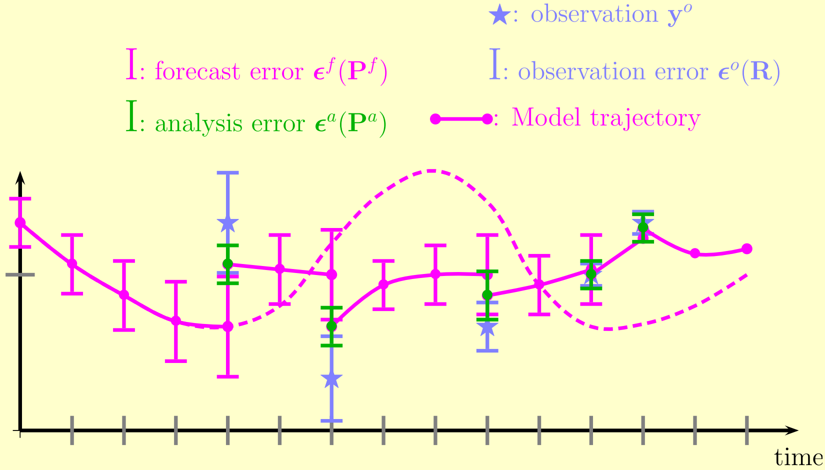
★: observation $\mathbf{y}^o$
I: forecast error $\boldsymbol{\epsilon}^f(\mathbf{P}^f)$
I: observation error $\boldsymbol{\epsilon}^o(\mathbf{R})$
I: analysis error $\boldsymbol{\epsilon}^a(\mathbf{P}^a)$
: Model trajectory
time

- Size of the covariance matrix: $n_\mathbf{x} \times n_\mathbf{x}$ ($n_\mathbf{x}$ is size of $\mathbf{x}$, typically 10^6).
- Evaluating $M\mathbf{P}_i^a M^\dagger$ requires $\mathcal{O}\left(n_\mathbf{x}^4\right)$ operations. ($n_\mathbf{x}$ times more expensive than a single model step.)

A 2-step procedure:

1. Forecast:

$$\mathbf{x}_{i+1}^f = M\mathbf{x}_i^a,$$

$$\mathbf{P}_{i+1}^f = M\mathbf{P}_i^a M^\dagger + \mathbf{Q}.$$

2. Analysis:

$$\mathbf{x}_{i+1}^a = \mathbf{x}_{i+1}^f + \mathbf{K}_{i+1}\left(\mathbf{y}_{i+1}^o - H\mathbf{x}_{i+1}^f\right),$$

$$\mathbf{P}_{i+1}^a = \left(I - \mathbf{K}_{i+1}H\right)\mathbf{P}_{i+1}^f.$$

with $\mathbf{K}_{i+1} = \mathbf{P}_{i+1}^f \mathbf{H}_{i+1}^\dagger \left(\mathbf{H}_{i+1}\mathbf{P}_{i+1}^f\mathbf{H}_{i+1}^\dagger + \mathbf{R}_{i+1}\right)^{-1}.$

- Possibility: use a frozen background error covariance matrix $\mathbf{P}^b$.

A 2-step procedure:

1. Forecast:

$$\mathbf{x}^f_{i+1} = M\mathbf{x}^a_i,$$
$$\mathbf{P}^f_{i+1} = \mathbf{P}^b$$

2. Analysis:

$$\mathbf{x}^a_{i+1} = \mathbf{x}^f_{i+1} + \mathbf{K}_{i+1}\left(\mathbf{y}^o_{i+1} - \mathbf{H}\mathbf{x}^f_{i+1}\right),$$
$$\mathbf{P}^a_{i+1} = \mathbf{P}^b$$

with $\mathbf{K}_{i+1} = \mathbf{P}^b\mathbf{H}^\dagger_{i+1}\left(\mathbf{H}_{i+1}\mathbf{P}^b\mathbf{H}^\dagger_{i+1} + \mathbf{R}_{i+1}\right)^{-1}$.

Structure of the background covariance matrix in 3D

Transport of information from the surface downwards:

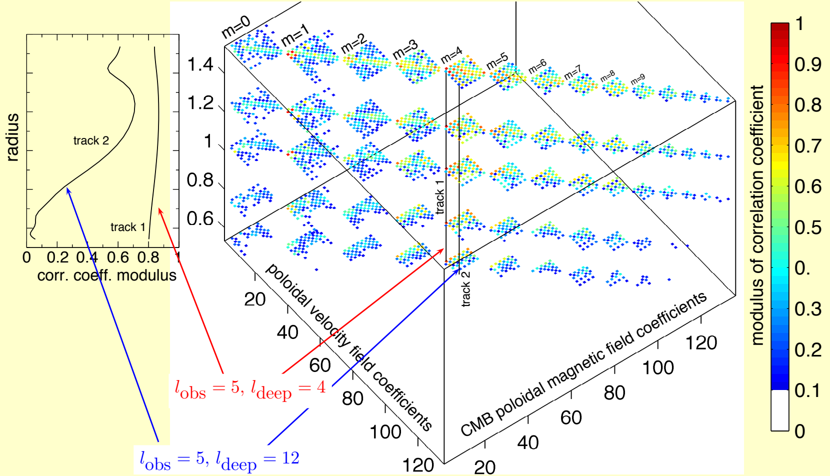

Aubert & Fournier, NPG, 2011

NB: several hundreds of samples are needed

Solve a time-dependent assimilation problem:

- Generate synthetic data from model free run over $[t_0, T]$: here maps of B_r at the top of the core (truncated at $\ell = 13$ and assuming perfect observations, $\mathbf{R} = \mathbf{0}$)
- Start from t_0 using wrong initial conditions (for instance the average background state)
- Assimilate synthetic observations and correct model trajectory
- Assess quality of assimilation scheme by comparing the known true dynamo state $\mathbf{x}^t$ and the estimate $\widehat{\mathbf{x}}$
  - Retrieval of internal structure
  - Forecast quality

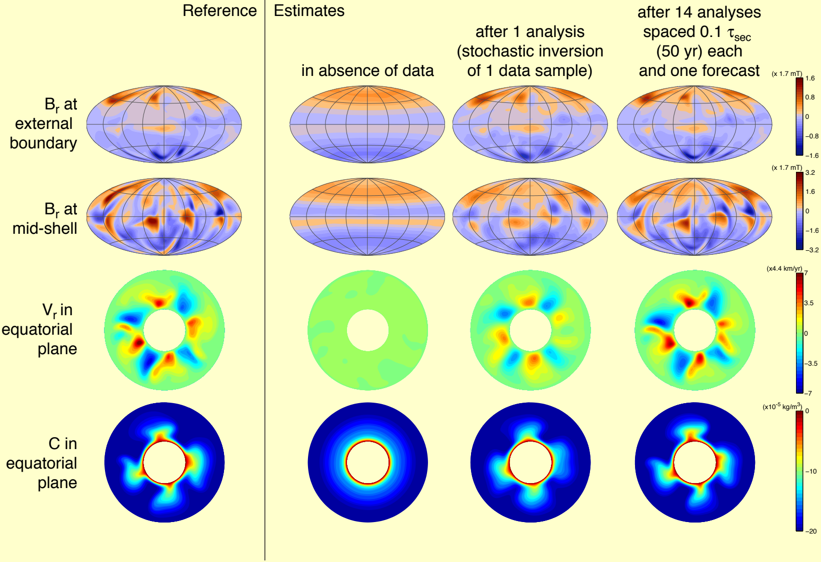

Aubert & Fournier, NPG, 2011

Forecast quality

Define the innovation

$$\mathbf{d}_i = \text{observation} \; - \; \text{forecast} = \mathbf{y}_i^o - \mathbf{H}\mathbf{x}_i^f$$

Involves the first 13 SH degrees of the poloidal field at the core surface.
Forecast quality via the average error

$$\text{error} = \frac{1}{N_{\text{cycles}}} \sum_i \|d_i\|_2 \text{ over 3000 yr}$$

The number of assimilation cycles N_{cycles} is set by the spacing between two successive cycles, Δt_{cycle}. We will take $\Delta t_{\text{cycle}} = 5$, 25, 50 and 100 yr.

Our forecast strategies to define $\mathbf{x}_i^f$ will consist of

1. a no-cast
2. a linear forecast based on the perfectly known SV up to SH degree 8
3. a linear forecast based on the perfectly known SV up to SH degree 13
4. a multivariate OI scheme assimilating B_r maps up to SH degree 13

Forecast results

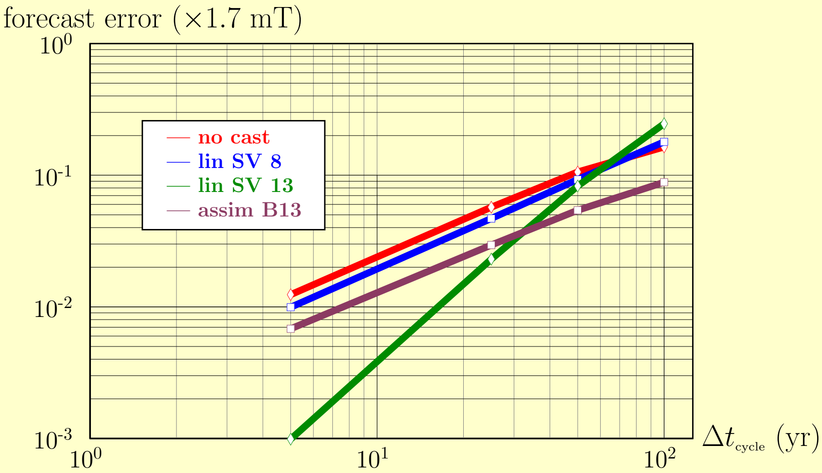

Over long time scales, assimilation provides the best answer.

It is of interest to elucidate the causes (and forecast the evolution) of the South Atlantic Anomaly.

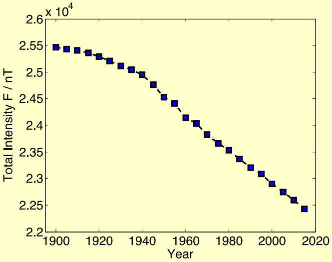

Finlay et al., 11th IGRF, GJI, 2011

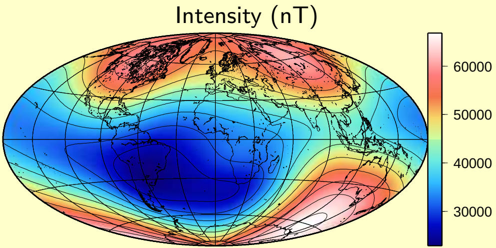

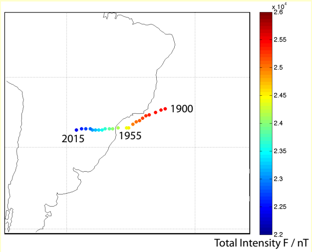

Finlay et al., 11th IGRF, GJI, 2011

Summary

- Implementation of an optimal interpolation scheme for geomagnetic data assimilation based on 3D models of the geodynamo
- Synthetic experiments:
  - Multivariate statistics help better constrain the internal structure of the core
  - Scheme adapted for long-term predictions of the evolution of the large-scale poloidal field at the top of the core
  - On short time scales: linear prediction based on perfectly well-known large scale SV performs better.

(ANR funded program for 2011-2015, http://avsgeomag.ipgp.fr)

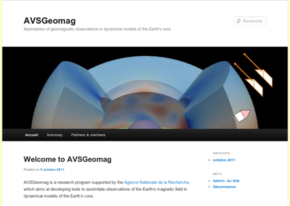

- Forward modelling: increase code performance (e.g. using GPUs)
  - Have time scales in better proportion
  - Equatorial dynamics
  - large-scale westward drift in a highly supercritical context
  - variability on short time scales (waves, etc.): better job than simple linear extrapolation
- Assimilation methodology
  - Incorporate uncertainties in scaling laws
  - Retrospective analysis: development of a smoother.
  - Highly nonlinear situation: EnKF, implicit particle filters ($$)